Synchronization patterns in transient spiral wave dynamics

Ulrich Parlitz, Alexander Schlemmer, and Stefan Luther

Max Planck Research Group Biomedical Physics, Max Planck Institute for Dynamics and Self-Organization, Am Fassberg 17, 37077 Göttingen, Germany and Institute for Nonlinear Dynamics, Georg-August-Universität Göttingen, Am Fassberg 17, 37077 Göttingen, Germany

(Received 17 February 2011; published 20 May 2011)

Transient dynamics of spiral waves in a two-dimensional Barkley model is shown to be governed by pattern formation processes resulting in regions of synchronized activity separated by moving interfaces. During the transient the number of internally synchronized regions decreases as synchronization fronts move to the boundary of the simulated area. This spatiotemporal transient dynamics in an excitable medium is detected and visualized by means of an analysis of the local periodicity and by evaluation of prediction errors across the spatial domain. During the (long) transient both analyses show patterns that must not be misinterpreted as any information about (spatial) structure of the underlying (completely homogeneous) system.

DOI: 10.1103/PhysRevE.83.057201 PACS number(s): 05.45.Xt, 05.45.Tp, 87.19.Hh

I. INTRODUCTION

Spatiotemporal systems in physics, biology, and other fields may generate complex dynamics whose characterization constitutes a major challenge in nonlinear dynamics and data analysis. An important class of systems exhibiting spatiotemporal dynamics is that of excitable media [1,2]. Excitable dynamics occurs mainly in chemical and biological systems. For example, in cardiac tissue electrical excitation waves are essential for proper contraction and pumping of the heart, where spiral waves or spatiotemporal chaos may lead to tachycardia or lethal fibrillation [3–5].

Relevant questions to be addressed when characterizing spatiotemporal dynamics are, for example: Is the underlying system spatially homogeneous or can it be divided into different regions governed by (slightly) different dynamics? Are there any "long-range interactions" connecting different parts of the full system? Is the observed dynamics chaotic or not, or is the system still in transient? A promising way to answer such questions is network analysis [6–11]. There, the system is observed (or measured) at different spatial locations and the resulting time series are investigated with respect to potential interrelations between different parts or regions of the system. Here different measures of interrelation may be employed, including linear cross correlation, (partial directed) coherence [12,13], mutual information [14–16], conditional entropy [17], transfer entropy [18], (cross) predictability [19–21] (similar to Granger causality [22]), or (phase) synchronization [23,24]. If strong relations are found this is often interpreted as being the result of structural inhomogeneities, hidden connections, or other causalities. In the following we shall present a numerical study showing that such conclusions can be misleading. Our system is a homogeneous excitable medium exhibiting periodic dynamics in terms of (multiple) spiral waves. Time series of this system are sampled on a (fine) grid of measurement points. To characterize the dynamics we use cross prediction between different locations (measurement grid points) by means of a nearest-neighbor predictor. Since the system is homogeneous with (global) periodic dynamics one would expect that all pairwise predictions provide similar errors. However, this is not the case. Instead we see some regions of low mutual prediction errors separated by borders across which relatively high prediction errors are obtained. The same patterns are observed when using mutual information for characterizing the network of measurements. The origin of these patterns is a rather slow transient process during which regions of the excitable medium adjust their dynamics by fine-tuning their oscillation periods. Once this synchronization transient is over, all patterns disappear and the network time series analysis provides the expected result (homogeneous cross-prediction errors). However, convergence to this asymptotic state is very slow. Therefore, in particular in experiments it is very likely that measurements are taken *during* the transient and may lead to wrong interpretations, for example concerning "inhomogeneity" of the underlying system or concerning additional connections between remote regions.

II. THE BARKLEY MODEL

As a model for demonstrating the synchronization transient and its implications for subsequent time series analysis we use the Barkley model. This qualitative model of an excitable medium was suggested in 1990 by Barkley *et al.* [25–27] and consists of a fast variable u and a slow inhibitory variable v described by partial differential equations,

$$\frac{\partial u}{\partial t} = \frac{1}{\varepsilon} u(1-u)\left(u - \frac{v+b}{a}\right) + \nabla^2 u, \tag{1}$$

$$\frac{\partial v}{\partial t} = u - v, \tag{2}$$

with three parameters: $\varepsilon = 0.02$ determines the time scale of the fast variable and $a = 0.8$ and $b = 0.02$ determine the excitation threshold and the action potential duration, respectively.

The Barkley model qualitatively describes various kinds of spiral wave dynamics [1,3,27] and has, for example, been used to demonstrate the unpinning mechanism upon far-field pacing of cardiac tissue [4,5]. With the parameters chosen here the system exhibits stable periodic spiral dynamics with (asymptotically) fixed spiral tips [27]. We consider a quadratic area of size $L \times L$ with $L = 100$. For numerically solving the Barkley model a spatial discretization using 200×200 grid points (with a five-point approximation of the Laplacian

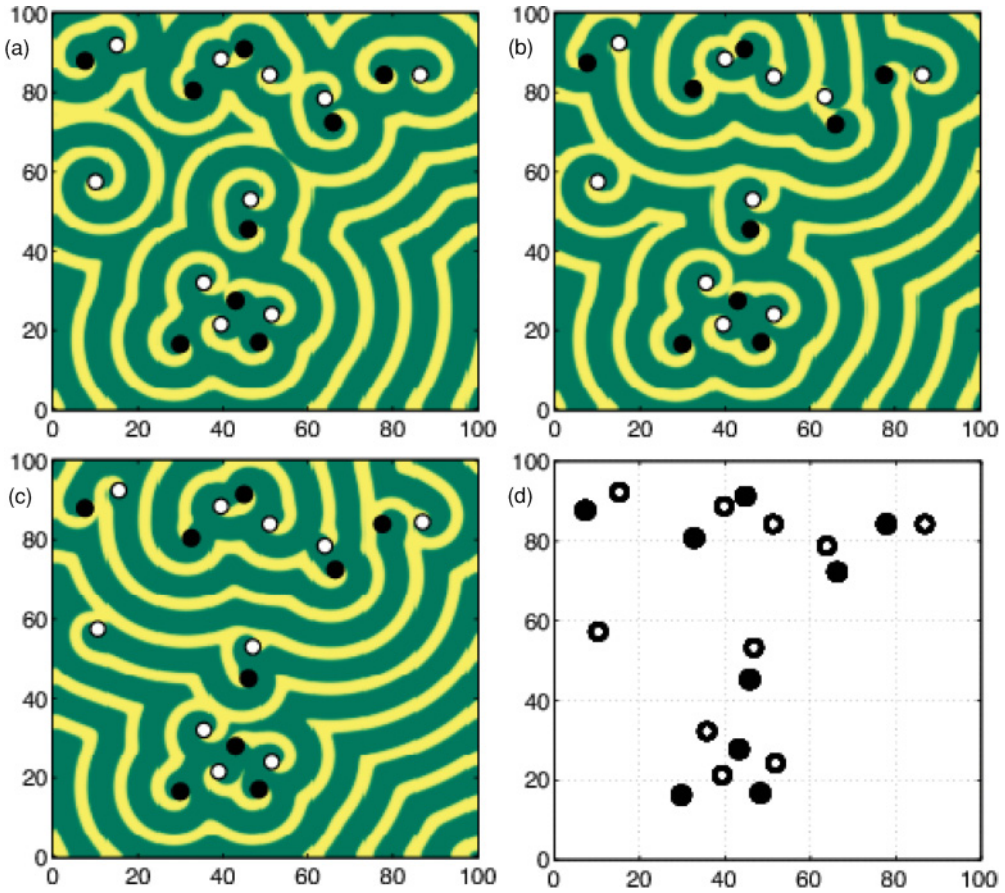

FIG. 1. (Color online) Snapshot of the periodic spatiotemporal dynamics generated by the Barkley model Eqs. (1) and (2) from random initial conditions at times (a) $t = 1{,}000$, (b) $t = 20{,}000$, and (c) $t = 30{,}000$. (d) Locations of spiral tips (phase singularities) for $1{,}000 < t < 50{,}000$. The circles indicate the position of phase singularities (open circles = clockwise rotation, filled circles = counterclockwise rotation).

operator) and Euler time steps of size $\Delta t = 0.02$ were used in combination with no flux boundary conditions.

When starting from different random initial conditions various configurations of stable spiral waves occur, all rotating with the same frequency. As an example for the resulting dynamics, Figs. 1(a)–1(c) show for random initial conditions snapshots at $t = 1{,}000$, $t = 20{,}000$, and $t = 30{,}000$. As can be seen, a system of interacting spiral waves occurs. Spirals rotate clockwise or counterclockwise, corresponding to the sign of the topological charges of the phase singularities at the spiral tips (indicate by filled and open circles in Fig. 1). For times $t > 1{,}000$ the locations of the spiral cores do not change any more, as can be seen in Fig. 1(d) where the positions (i.e., trajectories) of phase singularities are shown for the period of time of $1{,}000 < t < 50{,}000$. Figure 2 shows a typical example of the signal $s(t) = u(\mathbf{z},t)$ measured at location $\mathbf{z} = (40,42.5)$.

III. CROSS-PREDICTION DIAGRAMS

For characterizing the spatiotemporal dynamics we shall evaluate now its cross predictability between different locations. More precisely, it is checked how well the dynamics at some point B in space can be predicted using a time series from point A. Technically, this approach is implemented in terms of nearest-neighbor prediction [19]. There, at point A a time series $\{x_A(t_n)\}$ is sampled at times $t_n = nT_s$ and used to reconstruct d-dimensional states $\mathbf{x}_A(t_n) = [x_A(t_n), x_A(t_n - \tau), \ldots, x_A(t_n - (d-1)\tau)]$ with delay time τ. Then, for each time step t_n the nearest-neighbor $\mathbf{x}_A(p_n)$ of $\mathbf{x}_A(t_n)$ is determined with time index $p_n < t_n$ (i.e., a neighboring state occurring in the past). To predict the (current) time series value $y_B(t_n)$ at point B we use the (known) past value $y_B(p_n)$. This kind of nearest-neighbor prediction is repeated over N time steps to compute the mean prediction error:

$$E = \frac{1}{N}\sum_{n=1}^{N} |y(t_n) - y(p_n)|.$$

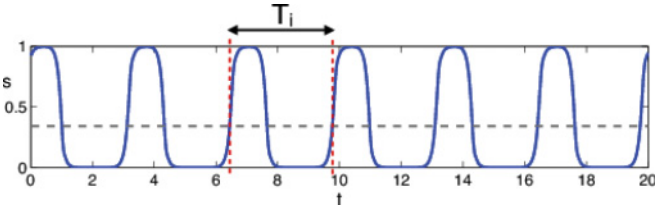

FIG. 2. (Color online) Typical local signal $s(t) = u(\mathbf{z},t)$ at spatial location $\mathbf{z} = (40,42.5)$ in the medium. The dashed horizontal line represents the mean value of the signal. Cross points of this line mark the beginning and the end of a period T_i of the oscillation.

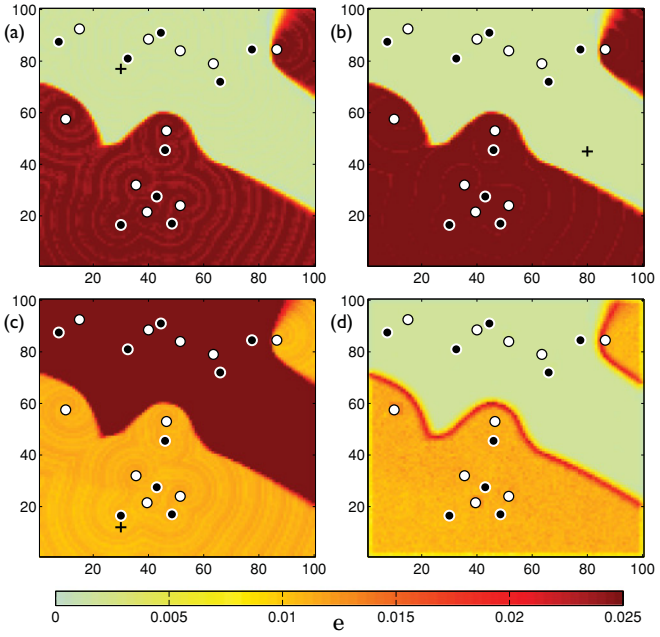

FIG. 3. (Color online) Predictability charts of the Barkley model at time $t = 20{,}000$. (a)–(c) Prediction error (color coded, see color bar at bottom) of different spatial locations when using forecasts from a given site indicated by +. (d) Boundary of the predictability regions obtained by local averaging the prediction error from any reference point to its 24 neighbors.

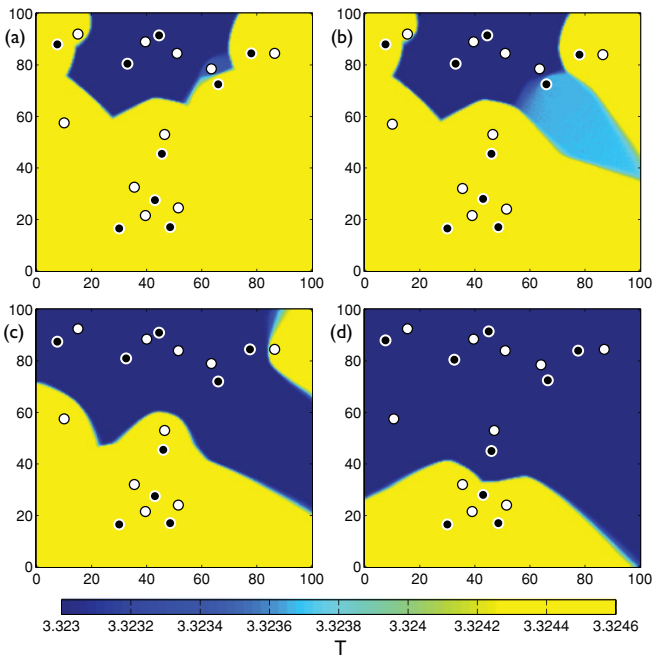

FIG. 4. (Color online) Color-coded local mean periods T at different times during the transient at times (a) $t = 10{,}000$, (b) $t = 11{,}000$, (c) $t = 20{,}000$, and (d) $t = 30{,}000$. The (filled) circles mark the locations of phase singularities (spiral tips), compare Figs. 1 and 3.

To normalize this error we estimate the forecasting error obtained with randomly selected neighbors (reconstructed state vectors):

$$E_R = \frac{1}{N}\sum_{n=1}^{N} |y(t_n) - y(q_n)|,$$

where $q_n \in \{1,\ldots,N\}$ is an integer random variable. The resulting relative prediction error

$$e = \frac{E}{E_R} = \frac{\sum_{n=1}^{N} |y(t_n) - y(p_n)|}{\sum_{n=1}^{N} |y(t_n) - y(q_n)|} \qquad (3)$$

ranges between 0 (perfect prediction) and 1 (prediction not better than random guessing).

Figure 3(a)shows the relative prediction errors from site A (indicated by the + symbol) to all other locations on a numerical grid with 100×100 sampling locations for $\tau = T_s = 0.4$, $d = 3$, and $N = 250$. As can be seen, there are essentially two regions where the prediction error is small or large, respectively. In Fig. 3(b) the same kind of diagram is shown for another reference point, where the same two regions occur as in Fig. 3(a). Figure 3(c) shows an example where the reference location (indicated by +) lies in the "other" region for which in Figs. 3(a) and 3(b) the prediction error was relatively high. As can be seen by comparing Fig. 3(c) with Figs. 3(a) and 3(b), regions of low predictability become more predictable and vice versa. Boundaries between predictability regions are clearly visible. To localize and plot the boundaries between such regions we average for each point in space the prediction error from this point to its 24 neighboring points on the grid. This average is small as long as the point lies within a predictability region but increases when the 24 neighboring grid points belong to different dynamical regions as can be seen in Fig. 3(d). In all diagrams shown in Fig. 3 the locations of spiral tips (phase singularities) are indicated by black and white circles (compare Fig. 1). The same patterns as those shown in Fig. 3 have also been obtained by computing the mutual information [14–16] of a given reference point and other locations in the square (where the mutual information is maximized with respect to time shift).

A particular feature of the predictability diagrams in Fig. 3 is the fact that the dark region in Figs. 3(a) and 3(b) [corresponding to the bright (orange) region of low prediction errors in Fig. 3(c)] consists of two separated parts. Without any additional knowledge about the underlying system one might conclude that there exists an additional (long-range) link connecting both separated regions and providing in this way the "remote" predictability shown in Fig. 3(c). Here we know that this interpretation is wrong (because the Barkley model is completely homogeneous) and may thus be viewed as an example of a possible pitfall of network analysis.

IV. PERIODICITY AND SYNCHRONIZATION TRANSIENT

The patterns occurring in the prediction diagrams in Fig. 3 turn out to be due to a (long) transient toward the asymptotic periodic dynamics. This transient is governed by a synchronization process of periodic oscillations of neighboring areas of the medium resulting in regions of synchronized activity separated by (moving) boundaries.

To characterize the synchronization (transient) we computed for each time series $s(t) = u(\mathbf{z},t)$ [sampled at point $\mathbf{z} = (z_1, z_2)$ on the measurement grid] its mean value $\bar{s}$ and

subtracted it from the time series. Then the zero crossings of the resulting signal $\tilde{s}(t) = s(t) - \bar{s}$ (with positive slope) were detected and used to compute a (instantaneous) period of the signal (at time t and location $\mathbf{z}$), see Fig. 2. These instantaneous periods were averaged for a time interval of length 100 from $t - 100$ to t and provide momentary local periods $T = T(\mathbf{z},t)$ that slowly converge to the asymptotic period of the full system. Figure 4 shows color-scaled charts of the momentary periods of the periodic oscillations [obtained from variable $u(\mathbf{z},t)$]. At this stage of the (synchronization) transient essentially two regions with slightly different periods (see color bar at the bottom of Fig. 4) exist. The dark (blue) region grows in time and finally the full square has a period of $T \approx 3.323$ (for $t > 39{,}000$, not shown here). The growth process is either continuous by means of a slowly moving boundary or consists of a collective transition of some subarea as visible in Figs. 4(a) and 4(b) (light blue/gray region). Comparison of the period diagram Fig. 4(c) with the prediction diagram Fig. 3 shows that regions and borders (considered at the same time t, here $t = 20{,}000$) coincide. As can be seen, minor variations of the (local) period (from $T = 3.3246$ to $T = 3.323$) result in a strong in- or decrease of the prediction error.

V. CONCLUSION

The main conclusions that one may draw from the presented simulation results are as follows:

(i) Convergence to periodic spiral wave dynamics in excitable media is governed by synchronized regions expanding continuously (with moving boundaries) as well as by transitions of extended regions [see, for example, the transition from Fig. 4(a) to Fig. 4(b)].

(ii) During this transient, data analysis methods evaluating interrelations of signals sampled at different spatial locations reflect and visualize this dynamical pattern (but must not be misinterpreted as information about the spatial structure of the underlying system).

We expect that both aspects not only are relevant for excitable media but also for other spatiotemporal systems exhibiting transient periodic dynamics. For extended chaotic systems, on the other hand, cross-prediction errors increase with the distance between measurement points. There, good predictability between two remote cites may indeed be interpreted as an indicator for a direct connection between both of those points due to an additional link. But still, differences in predictability (or similar measures, like mutual information) maybe due to dynamics only, without any inhomogeneity of the underlying (physical) system. This difference in the dynamics may be due to initial conditions (like with chimera states [28–30], for example) and/or represent a temporary phenomenon occurring during transients, only.

ACKNOWLEDGMENTS

The research leading to the results has received funding from the European Community's Seventh Framework Programme FP7/20072013 under grant agreement No. HEALTH-F2-2009-241526, EUTrigTreat. S.L. acknowledges support from the BMBF (FKZ 01EZ0905/6).

[1] A. T. Winfree, *The Geometry of Biological Time*, 2nd ed. (Springer, New York, 2010).
[2] M. Cross and H. Greenside, *Pattern Formation and Dynamics in Nonequilibrium System* (Cambridge University Press, Cambridge, United Kingdom, 2009).
[3] E. M. Cherry and F. H. Fenton, New J. Phys. **10**, 125016 (2008).
[4] P. Bittihn, G. Luther, E. Bodenschatz, V. Krinsky, U. Parlitz, and S. Luther, New J. Phys. **10**, 103012 (2008).
[5] P. Bittihn, A. Squires, G. Luther, E. Bodenschatz, V. Krinsky, U. Parlitz, and S. Luther, Philos. Trans. R. Soc. London A **368**, 2221 (2010).
[6] A. A. Tsonis and P. J. Roebber, Physica A **33**, 497 (2004).
[7] J. F. Donges, Y. Zou, N. Marwan, and J. Kurths, Europhys. Lett. **87**, 48007 (2009).
[8] J. F. Donges, Y. Zou, N. Marwan, and J. Kurths, Eur. Phys. J. Special Topics **174**, 157 (2009).
[9] N. Malik, N. Marwan, and J. Kurths, Nonlin. Processes Geophys. **17**, 371 (2010).
[10] K. Steinhaeuser, N. V. Cawla, and A. R. Ganguly, *Statistical Analysis and Data Mining*, (in press, 2010).
[11] S. Bialonski, M.-T. Horstmann, and K. Lehnertz, Chaos **20**, 013134 (2010).
[12] L. A. Baccal and K. Sameshima, Biol. Cybern. **84**, 463 (2001).
[13] M. Jachan, K. Henschel, J. Nawrath, A. Schad, J. Timmer, and B. Schelter, Phys. Rev. E **80**, 011138 (2009).
[14] R. Steuer, J. Kurths, C. O. Daub, J. Weise, and J. Selbig, Bioinformatics **18**, S231 (2002).
[15] K. Hlaváčková-Schindlera, M. Palus, M. Vejmelka, and J. Bhattacharya, Phys. Rep. **441**, 1 (2007).
[16] A. Kraskov, H. Stögbauer, and P. Grassberger, Phys. Rev. E **69**, 066138 (2004).
[17] A. Porta, G. Baselli, F. Lombardi, N. Montano, A. Malliani, and S. Cerutti, Biol. Cybern. **81**, 119 (1999).
[18] T. Schreiber, Phys. Rev. Lett. **85**, 461 (2000).
[19] M. Wiesenfeldt, U. Parlitz, and W. Lauterborn, Int. J. Bifurcation Chaos **11**(8), 2217 (2001).
[20] N. Ancona, D. Marinazzo, and S. Stramaglia, Phys. Rev. E **70**, 056221 (2004).
[21] L. Faes, A. Porta, and G. Nollo, Phys. Rev. E **78**, 026201 (2008).
[22] C. W. J. Granger, Econometrica **37**, 424 (1969).
[23] B. Schelter, M. Winterhalder, R. Dahlhaus, J. Kurths, and J. Timmer, Phys. Rev. Lett. **96**, 208103 (2006).
[24] B. Kralemann, L. Cimponeriu, M. G. Rosenblum, A. S. Pikovsky, and R. Mrowka, Phys. Rev. E **76**, 055201 (2007).
[25] D. Barkley, M. Kness, and L. S. Tuckerman, Phys. Rev. A **42**, 2489 (1990).
[26] D. Barkley, Physica D **49**, 61 (1991).
[27] D. Barkley, Scholarpedia **3**(11), 1877 (2008).
[28] Y. Kuramoto and D. Battogtokh, Nonlinear Phenom. Complex Syst. **5**, 380 (2002).
[29] D. M. Abrams and S. H. Strogatz, Phys. Rev. Lett. **93**, 174102 (2004).
[30] S. I. Shima and Y. Kuramoto, Phys. Rev. E **69**, 036213 (2004).